Yueping Yin · Yuliang Cheng · Jingtao Liang · Wenpei Wang

Heavy-rainfall-induced catastrophic rockslide-debris flow at Sanxicun, Dujiangyan, after the Wenchuan Ms 8.0 earthquake

Abstract This paper uses the catastrophic rockslide at Sanxicun village in Dujianyan city as an example to investigate the formation mechanism of a rapid and long run-out rockslide-debris flow of fractured/cracked slope, under the application of a rare heavy rainfall in July 2013. The slope site could be affected by the Wenchuan Ms 8.0 Earthquake in 2008. The sliding involved the thick fractured and layered rockmass with a gentle dip plane at Sanxicun. It had the following formation process: (1) toppling due to shear failure at a high-level position, (2) shoveling the accumulative layer below, (3) forming of debris flow of the highly weathered bottom rockmass, and (4) flooding downward along valley. The debris flow destroyed 11 houses and killed 166 people. The run-out distance was about 1200m, and the accumulative volume was 1.9×10^6m³. The rockslide can be divided into sliding source, shear-shoveling, and flow accumulative regions. The stability of this fractured rock slope and the sliding processes are discussed at four stages of cracking, creeping, separating, and residual accumulating, under the applications of hydrostatic pressure and uplift pressure. This research also investigates the safety factors under different situations. The double rheological model (F-V model) of the DAN-W software is utilized to simulate the kinematic and dynamic processes of the shear-shoveling region and debris flow. After the shear failure occurred at a high-level position of rock, the rockslide moved for approximately 47s downward along the valley with a maximum velocity of 35m/s. This is a typical rapid and long run-out rockslide. Finally, this paper concludes that the identification of the potential geological hazards at the Wenchuan mountain area is crucial to prevent catastrophic rockslide triggered by heavy rainfall. The identified geological hazards should be properly considered in the town planning of the reconstruction works.

Keywords Wenchuan Ms 8.0 earthquake ·
Heavy rainfall · Rockslide · Debris flow

Introduction

During July 7–12 of 2013, a heavy rainfall occurred at the Wenchuan Ms 8.0 earthquake area. The 5 days accumulative precipitation in the Dujiangyan area of Sichuan province was up to 1129 mm, which was rare in previous years and exceeded the mean annual precipitation of 1110 mm over the 25 years from 1987 to 2012. The heavy rainfall triggered a rapid and long run-out rockslide in Sanxicun village. Its debris had a volume of 1.9 million m³. It caused a sliding distance up to 1200 m and killed 166 people in the village. The Sanxicun landslide was located in Zhongxing town, Dujiangyan city of Sichuan province. The site is located at (E103°33′48″, N30°54′55″), 68 km away from Chengdu city to the east and 16 km away from the Dujiangyan urban district (Fig. 1).

This area was famous for its agreeable climate and beautiful natural mountain scenery, lakes, and abundant vegetation. The typical natural conditions to resorts and vocations often concealed the potentialities of rockslide, rockfall, and debris flow. This resulted in a misunderstanding in lower risk of geological hazards. This area enjoyed a high reputation stemming partly from the Qincheng Mountain–Dujianyan Scenic Resort and attracted a great many tourists every summer. Therefore, research on rainfall-induced post-earthquake geological hazards in these areas has significance to the reconstruction of towns and villages and the tourism safety after the earthquake. The rockslide dynamic response characteristics triggered by the Wenchuan Ms 8.0 earthquake and post-earthquake debris flow disaster have received much attention from researchers (Yin et al. 2009; Tang et al. 2011). Tang et al. (2009) reported a heavy-rainfall-induced debris flow disaster on September 24 of 2008 at the earthquake-ruined Beichuan town in the central part of the area affected by the Wenchuan Ms 8.0 earthquake and presented the possibility that, due to the ground shaking, the critical amount of accumulated precipitation and the hourly rainfall intensity necessary to initiate debris flow were reduced compared with values before the earthquake. Recently, Zhou and Tang (2013) summarized 11 rainfall events that induced debris flows between 2008 and 2012 after the Wenchuan earthquake and discussed the rainfall thresholds for debris flow occurrence. However, the researches on rainfall-induced rockslides after the earthquake and its transferring process into a long run-out debris flow have made little significant progress.

The parent rock of the Sanxicun rockslide is a slightly inclined, nearly horizontal strata sandstone formation with intact rock constitutes. This rockslide was located at southwest of Wenchuan Ms 8.0 earthquake fault and was only 12 km away from the epicentral region. The seismic intensity of the Sanxicun area was up to the IX degree. According to the emergency investigation 1 week after the Wenchuan Ms 8.0 earthquake, three small scale rockfalls were induced. Two rockfalls were at the frontier of the slope of the rockslide source area in the moving direction of NNE10°, and the other was at the southeastern corner in the moving direction of NWW288° (Fig. 2, also see Fig. 8). They presented a disturbance, or even damage on the slope from the earthquake. Research on this rockslide is significant for prevention on post-earthquake geological hazard prevention. Therefore, this paper uses the Sanxicun landslide as an example to study the stability of fractured slope after the Wenchuan Ms 8.0 earthquake and the formation mechanism of rapid and long run-out rockslides triggered by heavy rainfall. The adverse conditions of the geological features prior to the rockslide are investigated, which provide a scientific consideration for classifying hazard areas that should be subject to monitoring and prevention.

Environmental geological condition

In terms of geomorphology, the Sanxicun rockslide was located at the transition zone from the Chengdu Plain to the Qinghai–Tibet
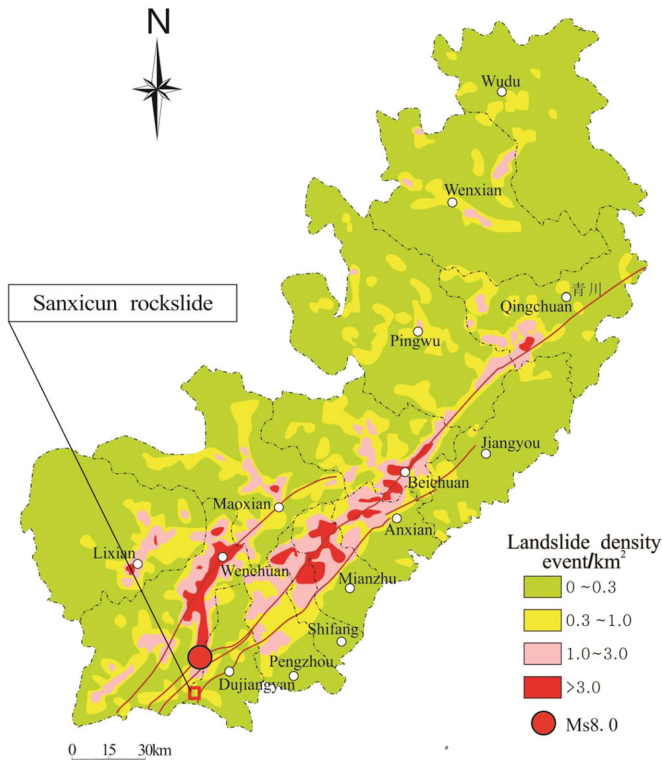
Fig. 1 Location of catastrophic rockslide-debris flow at Sanxicun, Dujiangyan due to heavy rainfall on July 10, 2013(also indicated map of density of landslides triggered by Wenchuan Ms 8.0 earthquake on May 12, 2008)

Plateau, which features erosion tectonics with low mountains and hills. Mountains generally run in the NE–SW direction with relatively flat peaks. The mountains are subject to the control of joint cracks in NE–SW and E–W directions. The northwest, northeast, and north of the mountains are free faces.

In terms of regional geology, the Sanxicun rockslide was located at the Longmenshan tectonic belt. It was on the SE side of the Erwangmiao secondary fault and the SE side of the Shenxianqiao

Fig. 2 3D images showing catastrophic rockslide-debris flow at Sanxicun (*red dashed line* indicates the small rockfall due to Ms 8.0 earthquake)

rear slope. The slope is a monoclinal structure mountain with a Cretaceous Guankou Formation (Kg) whose rock consists of brown-red and purplish red thick blanket sandstone, siltstone, and sandy mudstone.

With regards to precipitation, this area belongs to the middle semi-tropical moisture monsoon climate of the Sichuan Basin with abundant rainfall which is concentrated from May to September of every year. According to the 25-year precipitation statistics from 1987 to 2012, the mean annual precipitation is approximately 1100 mm. The precipitation from May to September accounts for 80 % of the annual rainfall, among which August has the maximum mean monthly precipitation of up to 243 mm (Fig. 3).

Field surveys on rockmass structure indicated that the parent rock of the Sanxicun rockslide was thick blanket sandstone and siltstone of the Cretaceous Guankou Formation (Kg) doped with small amounts of sandy mudstone. The bedding of the parent rock is 110°∠16°, indicating that it has a flat dipping bedrock slope. Remote sensing image presented that the rockslide body was cut into block structure by the three sets of preferred joints and a soft layer. The north and west sides of the rockslide body were free faces since its east one was obstructed by mountain. This resulted in a deflection in the principle slide direction from 110 ° (true dip angle) to the northeast direction (apparent dip angle). Figures 4 and 5 show the three sets of preferred joints in the rockslide and adjacent areas: (1) joint crack belt in NE–SW direction, (2) joint crack belt adjacent to E–W direction, and (3) joint crack belt adjacent to S–N direction. Combining joint crack direction and geomorphologic features, the first set of joint surfaces can be judged as inclined tension crack surfaces with a crack occurrence of 324°∠75–80°. The second set of joint surfaces can be judged as transverse tension crack surfaces, which are parallel to the rear tension surface and are known as "killing ditch" big cracks in residents with a crack occurrence of 3°∠86°. The third set of joint crack surfaces can be judged as longitudinal tension crack surfaces with a crack occurrence of 288°∠70–80°. The length of joint cracks in rockslide and adjacent areas is between 10 and 60 m. The numbers of the above three sets of joint cracks are more than 70 % in total, which reflects the preferred controlling characteristics on rockslide body, and the lower microrelief also reflected the consistency along the joint cracks.

Basic characteristics of rockslide

The Sanxicun rockslide was a gently inclined laminated rockslide. It is hard to know previously the failure of rockslide in the area due to the heavy vegetation coverage. The remote sensing images before and after the sliding are compared to analyze the extent of the slope failure effectively. Sheared at a high-level position, the rockmass was transferred to a rockfall and shoveled the bottom accumulative layer as well as severely weathered rock. The slide movement direction deflected 67° from 57° NE to 10° NW due to the obstruction of the front slope. Under the application of rainfall runoff, the rockfall crushed the valley downstream in the form of a flow rockslide, destroyed 11 houses located in the valley and adjacent tourism area, and killed/buried 166 people.

The elevations of rear edge and front accumulative area are 1140 and 720 m, respectively, which indicates an elevation difference of up to 420 m between the rear edge and front edge. The rockslide width had a maximum value of 420 m and a minimum value of 30 m. The rockslide had a longitudinal length of approximately
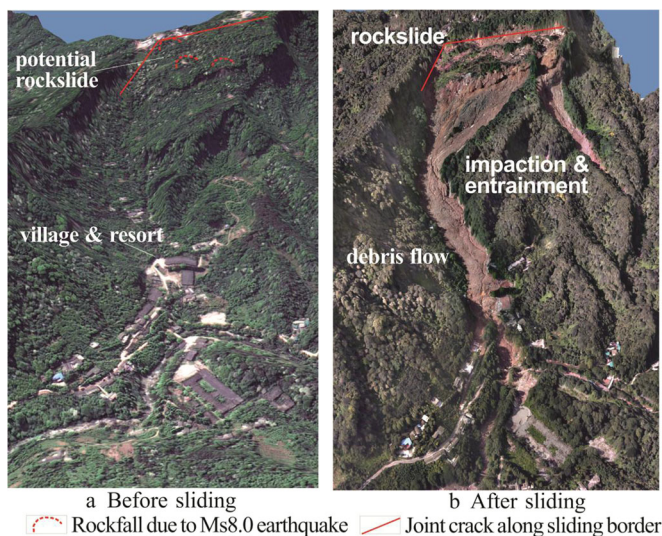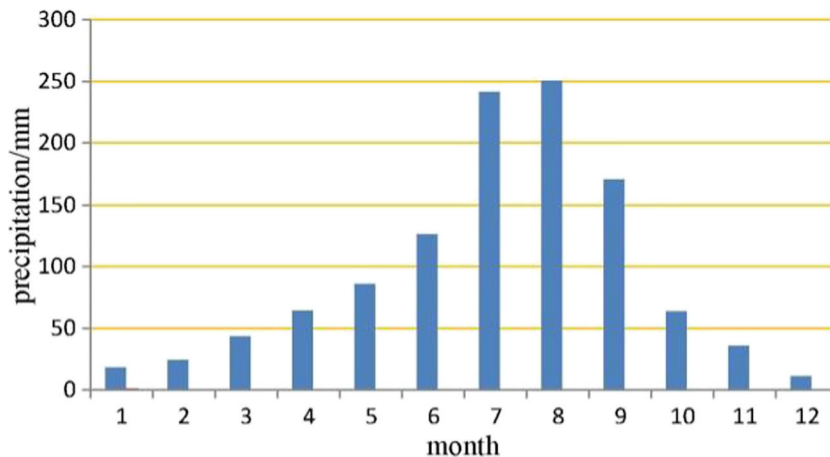
1200 m, and the rockslide area was 18.1×10^3 m². The maximum thickness of the rockslide accumulation was 30 m with a mean thickness of 10 m and a volume of 1.915×10^6 m³. The movement and accumulative characteristics of the rockslide can be classified into rockslide source area, impact-shoveling area, and flow accumulative area (Figs. 6 and 7) that will be described in detail in the following three paragraphs.

Rockslide source area

Rockslide source area was located approximately 100 m northwest from the downside slope of the Shangqing Palace Building in the Qingcheng Mountain Scenery Area. The terrain of this area is steep with a slope of approximately 30°. This area mainly consists of sandstone and siltstone. The surface is comprised of clay gravel soil covered by a Quaternary loose residual layer with a thickness of <2 m.

The boundaries of the east and the west and the rear edge of the rockslide were controlled by joints, the frontier was a free face (Fig. 8). The plane configuration of this area is an approximate parallelogram whose sections exhibit trapezoidal shapes with a larger thickness of rear part and a smaller thickness of front part. The elevation difference between the rockslide rear edge and the shear outlet is 96 m with an elevation of 1140 m for the former and 1044 m for the latter. The thickness of this area ranges between 30

and 54 m with a mean thickness of 40 m. The longitudinal length of this area ranges between 50 and 200 m with a mean value of 100 m. The plane of this area exhibits an irregular trapezoidal shape whose width is between 250 and 420 m with a mean value of 335 m. The mean area is 33.5×10^3 m², and the estimated volume is 1.47×10^6 m³.

After the sliding, the parent rock of rockslide only partially separated and retained the structural characteristics of rock. To estimate the volume of the rockslide accumulation, the enlarged index (I_e) is applied, i.e., the I_e is suggested that the volume of the accumulation is about 1.2–1.4 times the volume of the original rockmass of the rockslide (Yin et al. 2011). Therefore, by multiplying with a rockmass loose factor of 1.2, the accumulative volume of the rockslide source area can be computed as $1.2 \times 1.47 \times 10^6$ m³$=1.77 \times 10^6$ m³.

According to the estimate from remote sensing images prior and post-sliding, the entirety of the rockslide body moved downward about 50 to 80 m. A sliding mass with a volume of approximately 300×10^3 m³ was sheared out at a high-level position and moved along two directions, forming a major slide area and a branch slide area. The major slide moved along the N57° E direction with an estimated volume of 275×10^3 m³ and transferred to debris flow with a run-out distance of >1000 m from the exit of rockslide (also see Figs. 6 and 7). The major slide resulted in severe disaster and is the focus of this paper. The branch slide moved along the 10° NW direction with a flow distance of 380 m, a mean

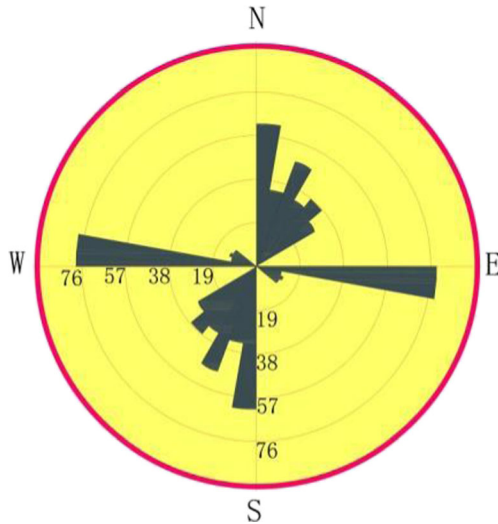**Fig. 4** Joint length and percentage in and around the Sanxicun rockslide
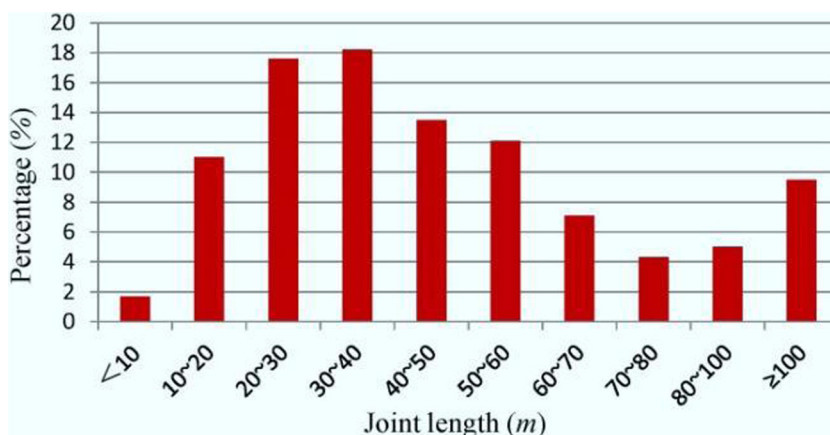
Fig. 5 Joint preferred direction in and around the Sanxicun rockslide

width of 65 m, an accumulative thickness of 1 m, and an estimated volume of 25×10³ m³. The branch slide area did not result in disaster, which is not the focus of this paper.

The residual accumulation volume of the rockslide was approximately 1.47×10⁶ m³. Two evident dips were formed at the rear edge and in the middle of the rockslide, which exhibited multiple imbricate slide features of rock. The rear edge dip was created by propagation and shearing application of the original cracks. The cracks were extended into a depth of 30 m, width of 64 m, and length of 350 m along the NW–SE direction (Fig. 9, also see Fig. 8) from a width of 4–8 m, depth of 8 m, and length of 180 m. The middle dip of the slope had a depth of 5–8 m, a width of 10–20 m, and an arch extension with a length of 160 m. Although the middle rockmass remained better rock structure, multiple tension cracks were developed with evident sinking features.

Impact-shoveling area

After being sheared at a high-level position, the major ditch area with a volume of 275×10³ m³ moved down along the N57° E direction and was accelerated by passing a 20-m high fault scarp. The rockslide was accordingly impacted to break and shovel the top 2-m thick surface rockmass and vegetation. This resulted in a triangle shoveling slope surface along the east side of the valley with a length of 380 m, an upper edge width of 280 m, and a front toe edge of only 60 m. The shoveled volume was about 119×10³ m³ and increased the rockslide volume (also see Fig. 8). The remaining residual accumulation with a volume of 60×10³ m³ at the impact-shoveling area moved downward forming a debris flow with a volume of approximately 335×10³ m³. The upper edge elevation of the impact-shoveling area was approximately 1024 m, and the front toe edge elevation was about 840 m (an 84 m difference).

The slope angle of the impact-shoveling area was 27° in average, up to 47° or steeper near the exiting zone of rockslide, which was beneficial to rapid sliding. Subjected to direction turning from the front valley, the debris flow of rockslide directly impacted the right side of the valley, which forced the rockslide to move with a 20° deflection and in an approximately northward direction.

Flow-accumulative area

Debris flow with an approximate volume of 335×10³ m³ moved down towards the valley in a NW direction. The length of the valley is about 650 m. The upper edge elevation of the valley was approximately 840 m, and the front toe edge elevation was about 740 m (an elevation difference of 100 m). The slope angle of valley had a maximum of 15°, and the corresponding terrain turned relatively flat. The valley features a seasonal water flow creek. Its water supplement is mainly from atmospheric precipitation, which controls the amount of water in the valley. In general, the valley has the water flow characteristics of a creek with intensive seasonal rise and fall. During July 8–10 of 2013, a heavy rainfall occurred in the valley and formed mountain torrents. It is estimated that the flow rate of the torrents was up to 5 m³/s. Therefore, after flooding, soil and mud joined the rock flow, and the rockslide turned into debris flow. The resultant debris flow accumulated along valley beds. According to site exploration report for the emergency prevention on debris flow (Figs. 10 and 11), the accumulation mainly consisted of huge rocks, stones, boulders, and silt clay. The content of huge rocks and boulders comprised approximately 25 % with a dominant size of 0.5 m and a maximum size up to several meters. The accumulation had a maximum thickness of
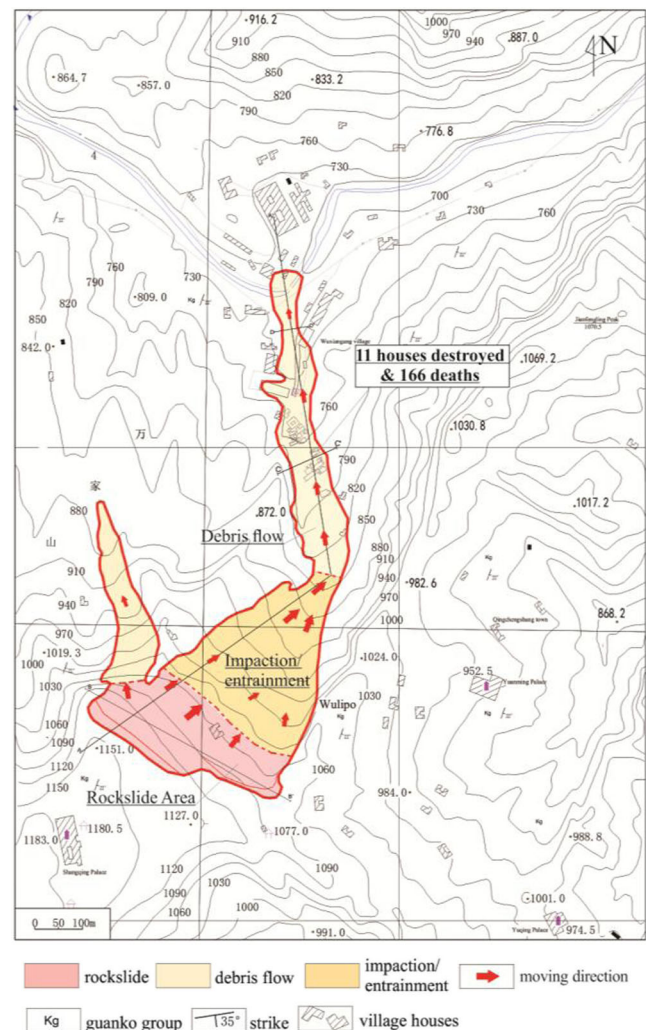

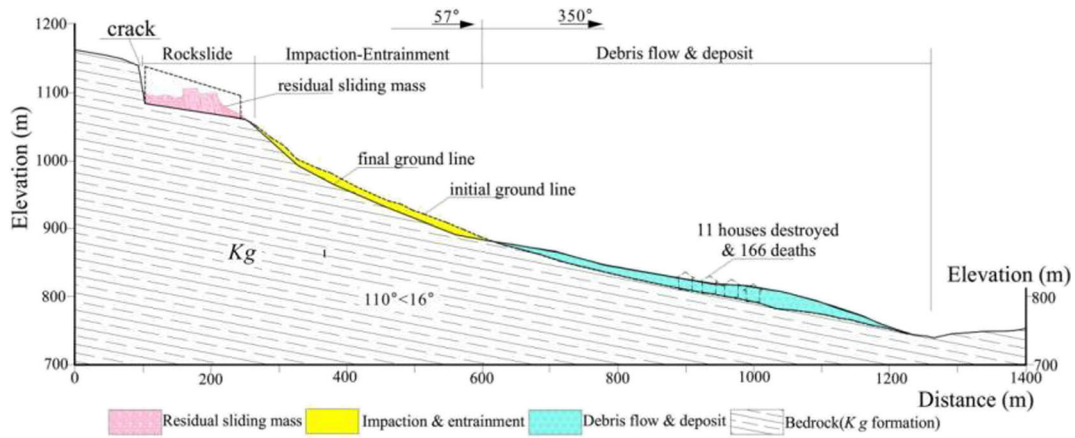Fig. 6 Map of Sanxicun rockslide-debris flow

Fig. 7 Longitudinal profile of rockslide-debris flow at Sanxicun

8 m with a mean value of 6 m, a width of 60–110 m with mean value of 90 m, an approximate area of 60×10^3 m^2, and an approximate volume of 360×10^3 m^3.

Initiation mechanism of rockslide

The front of the rockslide source area had a scarp with an elevation difference more than 20 m (NNE direction). The west side of the rockslide source area was a deep cut valley. The upper boundary of the rockslide source area was a tension fracture created by preferred joints along the NWW–SEE direction. It was recorded in the literature that this crack had been formed 400 years ago and had a maximum width of 10 m and a visible depth of up to 25 m (Fig. 12a) (Li 1998). After sliding, the maximum continuous extension length of this fracture was 250 m, and the width was 64 m (Fig. 12b). There were several tension cracks parallel to the "killing ditch" in the residues of the rockslide. These cracks had lengths of up to 100 m, splitting rocks into multiple blocks. The east boundary of the rockslide extended to the NNE–NE direction joints along the valley (also see Figs. 6 and 8). The rockslide was

obviously separated by two sets of dominate steep joints with discontinued interface and soft layer in bedrock that had an attitude of 110°∠16°. One was "tense joint" nearly vertical to the strike of the bedrock with smooth-jointed surface with an attitude of 3°∠86°. The other was a "compressive joint" nearly parallel to the strike of bedrock with an attitude varied between 288°∠70–80° and 324°∠75–80°. Due to the barrier of stable bedrock at the east boundary, a compressional area was formed at the southeast corner where the east boundary interconnected with rear edge cracks. This compressional area blocked the movement of rockslide along the direction of the true dip angle and forced a deflection of sliding direction from 110° SE to 57° NE, which formed a rockslide with an inclined dip azimuth. In other word, the rockslide was forced to change the movement direction into an apparent dip of NE from the true dip of SEE (also see Fig. 8 and 15). This kind of slide was typically studied taking a case of the Jiweishan rockslide at Wulong, Chongqing city, which occurred on June 5, 2009, illustrating a typical failure pattern of massive rock slope that rockmass rapidly slides along apparent dip, and then
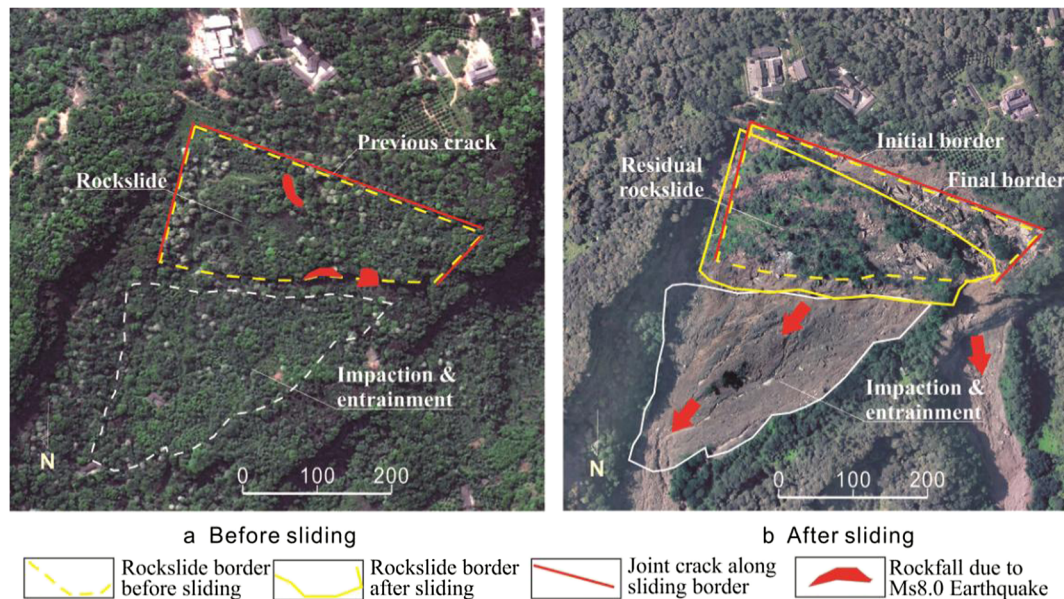

Fig. 8 RS images showing initial and final border of rockslide at Sanxicun

Fig. 9 Previous crack at back border of rockslide at Sanxicun (also see Fig. 8)

transforms into a long run-out rock avalanche (fragment flow). Before the Jiweishan rockslide, the failure pattern of an oblique inclined bedding slope was conventionally recognized as a lateral rockfall/topple and then a transformation into a rockfall accumulation landslide (Yin 2011; Feng et al. 2012). There were several sets of bedding silt lamellar shatter zones in the rockmass (with occurrence of 110∠16°), which cut and separated the sliding rockmass from the parent rock at the slope bottom to form the bottom sliding face. At the initial stage of rockslide deformation, the weak layer and surrounding rock layers were relatively complete due to no obvious dislocation, which was resisting to groundwater (Fig. 13a). During the creeping or sliding of rockslide, that brittle weak layer and surrounding rock layers were fractured or cracked, which provided a pass way to flow and an aquifer to storage of groundwater (Fig. 13b). The uplift pressure on the bottom of rockslide was created because the zones provided beneficial conditions for groundwater preservation and runoffs.

Starting at 2000 hours, July 8th 2013, a regional heavy rainfall occurred in Dujiangyan area. This strong rain featured long duration, a wide scope of influence, and severe hazard. The heaviest rains occurred between 2000 hours, July 8th, and 2000 hours, July 10th. During this time period (2 days long), the rainfall at 35

monitoring stations of Dujiangyan all reached above 250 mm, the monitored rainfall at the other 12 stations exceeded 500 mm, and the accumulated maximum precipitation was 1059 mm. This heavy rainfall achieved a historic record. It has been the heaviest rainfall since 1954 when Dujiangyan began to record meteorological data (Fig. 14).

Apparently, during this long-term heavy rainfall, a great deal of rain infiltrated into the rear edge tension fractures along the rockslide and generated hydrostatic pressure. Meanwhile, groundwater also infiltrated into rockmass along the gentle dip fractured rockmass to produce water head pressure. These processes deteriorated the deformation of rockmass along the dip angle and resulted in the separation of rockmass and the shear failure at a high-level position. Many investigators have studied the rockslide trigger mechanism of gentle dip-horizontal rockmass and proposed a sliding mechanism jointly driven by hydrostatic pressure at the rear edge inclined fractures and uplift pressure at the bottom surface as a result of groundwater infiltration (Ji et al. 2000; Fan et al. 2009). Of course, some scholars did not agree with this view for that the idea of a significant fluid pressure in a tension crack is likely not very real. First of all, it is hard to imagine that a tension crack could hold water for any period of time. Secondly, the volume of water in a narrow tension crack could be very small, so any slight lateral movement of the sliding mass would result in an immediately disappearance of the water and the associated lateral force. Thus, considerable thought has to be given to whether a tension crack filled with water can actually exist, and if it can exist, would the lateral hydraulic force remain when there is some as movement (GEO-SLOPE International Ltd. 2008).

The Sanxicun rockslide met the two conditions mentioned above. First, it must be noted that the section cut along a true dip angle of 110° of rockmass (Fig. 15, also see Fig. 6) that was basically parallel to the rear edge tension fracture. The highest ground point prior to sliding was located at the west boundary at an elevation of 1125 m, and the lowest ground point was at the east boundary at an elevation of 1050 m. There was an elevation difference of 75 m between these two ground points. The east boundary was not only the slide-blocking boundary but also the water barrier for groundwater due to the compression of rockslide movement along true dip at the early stage. This configuration

Fig. 10 Cross-section of debris deposit at Sanxicun (C–C') (also see Fig. 6 for the section layout)
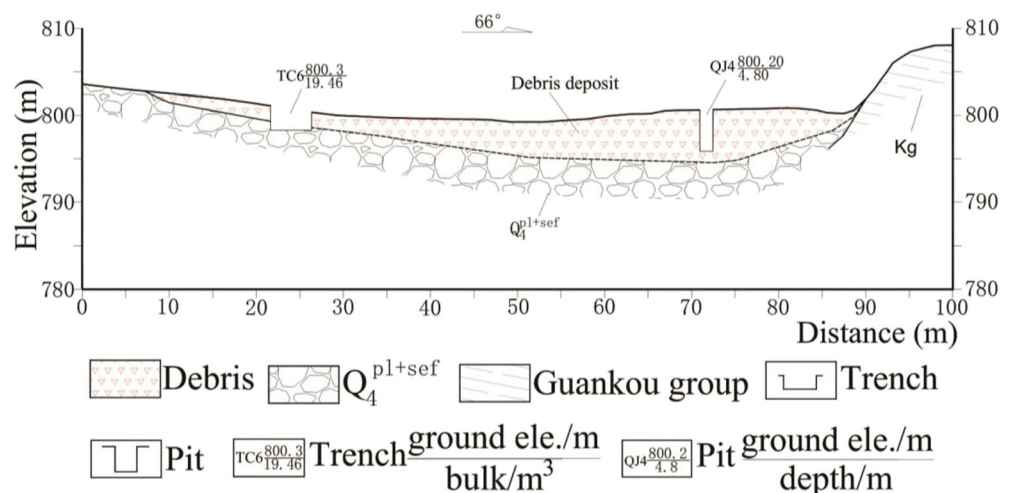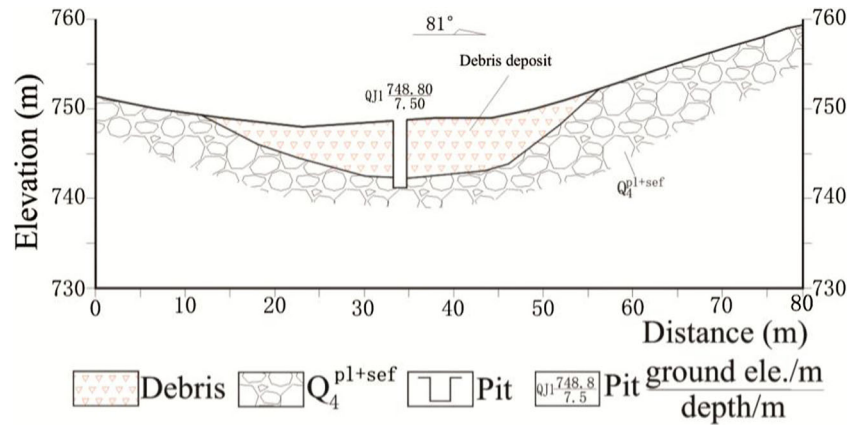
Fig. 11 Cross-section of debris deposit at Sanxicun (D–D')(also see Fig. 6 for the section layout)

assured that the groundwater in rear edge tension fracture could steadily reach the needed height before sliding and at the early stage of sliding. It could be speculated from Fig. 15 that the groundwater in the tension fracture could keep a relatively steady depth due to a closed hydrogeological condition not easily yielding to discharge formed by the oblique apparent dip layered rockmass. Secondly, the heavy rainfall before and during the rockslide not only exceeded the record of recent decades but also created a duration record. This kind of continuous several-days-long extreme heavy rainfall was enough to provide the necessary groundwater lastly recharge and seepage into the crack during the rockmass sliding. Thus, the slide of the rockmass could be generalized into four stages of cracking, creeping, separating, and residual accumulation (Fig. 16).

Cracking stage

This stage corresponded to the early process of rock crack deformation. Due to the incised valley, a terrain with two free faces was formed surrounding the east and north sides of the slope. Multiple sets of joints resulted in unloading cracks in the rock. These unloading cracks on the track of large joints in the NWW–SEE direction of the rear edge then formed preferred tension cracks. Meanwhile, there was no evident slide in the weak layer consisting of siltstone and shall sandstone at the bottom of the rock. During the rainfall, surface water infiltrated into the rockmass along steep inclined cracks at the rear edge, which produced hydrostatic

pressure on the rear edge of rockmass. However, the gently inclined cracks along the bottom of the rockmass were not well developed and had poor water permeability; therefore, penetrating uplift pressure could not occur (Fig. 16a).

Due to a lack of groundwater and runoff information in the rockslide, it is difficult to set up the seepage field in the rockmass. The 2D analysis on typical longitudinal section is preferred instead of 3D numerical simulation. This paper utilizes the Geo-Studio 2007 commercial software to simulate the stability of rockmass under the application of hydrostatic pressure in the relaxed crack stage (Swedish method of slices). Rockslide of the Cretaceous Guankou Formation has a wide distribution in the Sichuan area, which makes it possible to select parameters in an analogy method. This paper selects a typical strength testing index of saturated rockslide soil recommended by the Rockslide Investigation Report at Fenghuangshan, Chengdu (Zhao et al. 2009) which includes:

1. Shear strength for sliding surface(clay): cohesion c=13.54 kPa and internal friction angle Φ=8.74°
2. Rockslide mass(mud rock): cohesion c=70–100 kPa; internal friction angle Φ=20–42°; density γ=21 kN/m³.

A calculated model is conceptualized according to the hydrogeological condition and rockmass structure, in which the size of model has the same size as the actual rockslide with a longitudinal length of about 140.6 m and a height varying from 55.6 to 34.7 m
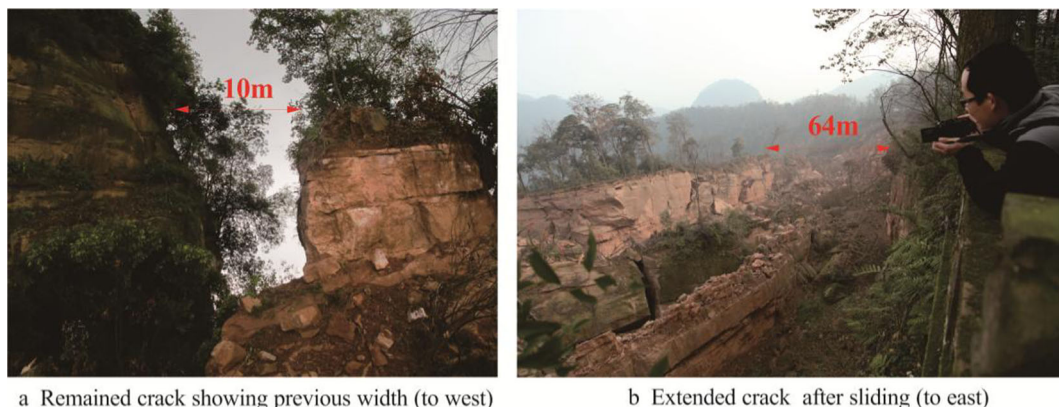

a Remained crack showing previous width (to west)

b Extended crack after sliding (to east)

Fig. 12 Photos showing the width of back crack of rockslide before and after sliding

a Brittle weak layer for sliding zone of rockslide   b Broken layered rockmass of sliding zone
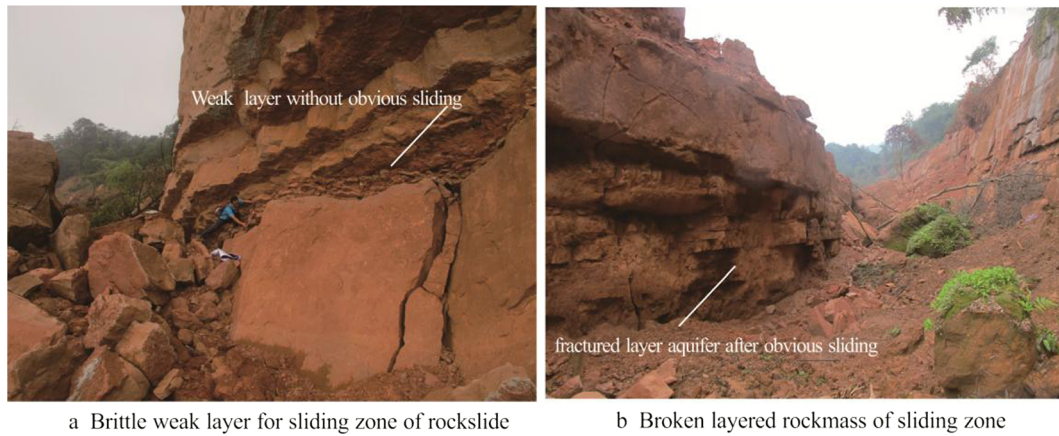
Fig. 13 Fractured rockmass showing a rich water-bearing layer

(Fig. 17, also see Fig. 7). The model has three sub-blocks at the stages of cracking and creeping, and then front block sliding away according to the remote sensing images. Since the water level that filled in tension cracks of rockmass during the rainfall has not been actually tested, an approximate method using the percentage ratio of filling level to crack thickness is used for trend analysis.

When cracks are not filled with groundwater, the factor of safety (FOS) equaled 1.105 (Table 1), which indicates that rockmass is generally stable. However, the rear edge of rockmass is subject to hydrostatic pressure with the increase in the filling depth of groundwater. The corresponding safety factor decreases. When the filling depth (h) of groundwater reaches 60 % of the tension crack thickness at the rear edge of rock, the hydrostatic pressure (P_s) applied to the rear edge of rockmass can be determined by the equation:

$$P_s = \gamma h^2/2 = 10 \times 32.4^2/2 = 5248.8 \text{ kN/m}$$

Under this situation, the FOS equaled 1.007, and the rockmass is at the critical slide status.

Creeping stage

This stage corresponded to the evolution process that the steep inclined joints separated from adjacent parent rock and cracked rockmass transformed into sliding mass. A weak zone with good property of water penetration was formed due to the long-term movement of the weak bottom layers along the inclined direction. The penetration of rain along the steep inclined cracks produced hydrostatic pressure, which applied to the rear edge of sliding mass and also formed uniform uplift pressure. This uplift pressure resulted from the evident slide at the bottom weak zone. The pressure was applied to the free face area from the rear edge to the front edge of sliding mass, where there was a certain thickness of gentle inclined crack zone and good water permeability (Fig. 16b, also see Fig. 12b).

The sliding mass was simultaneously subject to the application of rear edge hydrostatic pressure (P_s) and bottom uplift pressure (P_u) (Fig. 18 and Table 1).

When the filling depth (h) of groundwater reached 60 % of the rear edge tension crack thickness (H), the sliding mass was subject to not only hydrostatic pressure of 5248.8 kN/m at rear edge but also to uplift pressure at the bottom with a value determined according to the following equation:

$$P_u = \gamma hl = 10 \times 32.4 \times 150 = 48,600 \text{ kN/m}$$

This situation corresponds to a FOS equal to 0.819 and a sliding status. This superposition effect results in an evidently lower FOS. Actually, under joint application of hydrostatic pressure and uplift, if the filling depth of groundwater exceeds 20 % of the crack depth

Fig. 14 Diagram of heavy rainfall at Dujiangyan from June 15 to July 19 of 2013
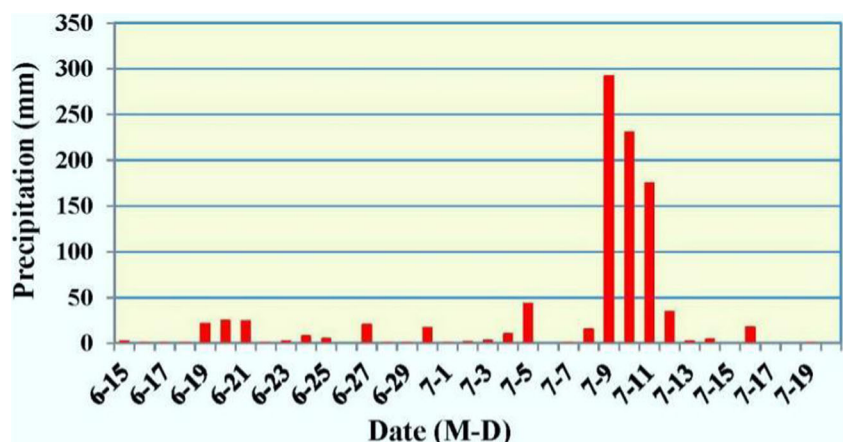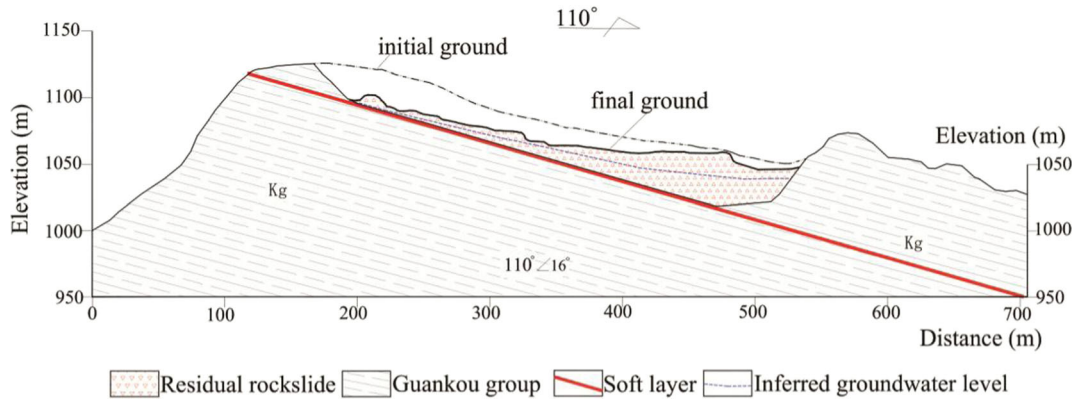
Fig. 15 Dip-direction profile section of rockslide at Sanxicun

(H) of the rear edge, i.e., 11 m, FOS would be equal to 1.0 and sliding would occur.

Separating stage

This stage corresponds to the evolution process of an evident slide, gradual failure of rock, separation from parent rock, and rockslide formation. Multiple steep inclined joints developed, continued to cut the slide mass into multiple blocks, and resulted in separation of the slide mass. Especially at the steep location with free faces at the front edges, the rockmass was readily sheared to rockslide failure at a high-level position, the front rockslide changed to fall, topple, or rotate (Fig. 16c). Rainfall infiltrated into rockmass through a variety of steep inclined cracks and produced multiple sections of hydrostatic pressure. Meanwhile, the uniform uplift pressure applied in the free face area from the rear edge to the front edge at the bottom gentle dip laminated crushing zone produced multiple sections of uplift pressure. Many investigators studied the characteristics of groundwater pressure in the multiple cracks. With the physical simulation, Xu et al. (2012) conducted a research on the deformation and failure evolution of the translational rockslide, which was caused by the cooperation of the hydrostatic pressure and the uplift pressure. The clear relationship

between the critical water head and the dip angle of the sliding plane was revealed in the results: The larger the dip angle of the slide plane was, the smaller the critical head would be under the same physico-mechanical parameters of rock and soil in the rockslide. Wang et al. (2012) presented a similar result that the wedge-shaped cracking expansive force of groundwater played a key role in the course of deformation and destruction of slope for the near horizontal layered rock slope.

In the early stage of rock separation, the cracks in sliding mass were not filled by groundwater. Therefore, the bottom uplift pressure generally exhibited a triangle distribution, i.e., $P_u = \gamma hl$ (Fig. 19a). With the increase in movement, the rockslide was gradually separated, and the wedging expansion from the groundwater in cracks correspondingly increased and expanded. This resulted in the bottom uplift pressure changing overall and exhibiting a composition distribution of a trapezoid and triangle (Fig. 19b, also see Fig. 16c), i.e.

$$P_u = \gamma[(h_1 + h_2)l_1/2 + h(l - l_1)]$$

Under the condition of rockmass cracking, a special situation of $h_2 = h_1$ might occur in which the uplift pressure applied on the rear

Fig. 16 Sliding pattern of cracked layered rockmass under water pressure
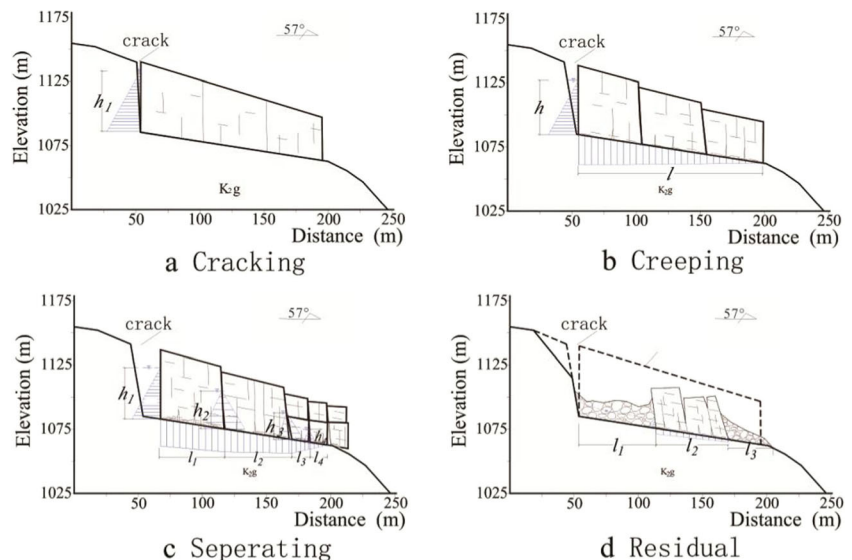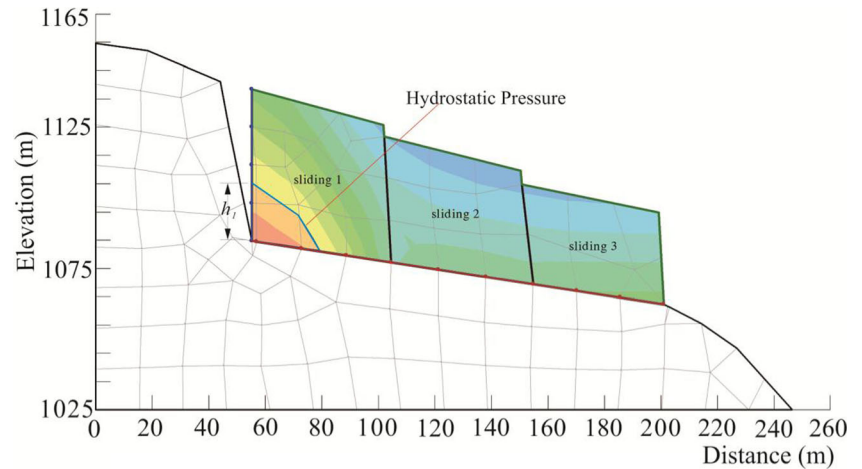
Fig. 17 Seepage analysis with hydrostatic pressure (cracking stage)

block varies from trapezoid to rectangular, and the safety factor decreased accordingly (Table 2).

It must be noted that during sliding, separation of rockmass structure was accelerated, and the discharge of groundwater was accomplished more readily. Accordingly, the groundwater hydrostatic pressure at the tension cracks of the rear edge and the uplift pressure at the bottom cracked rockmass decreased significantly.

Residual accumulating stage

This stage corresponds to the process that the decrease in groundwater hydrostatic pressure after the shear failure of rockmass resulted in a slow slide of material on a gentle dip surface (Fig. 16d). In the process of a large slide, rockmass further separated to stone blocks. The major application of groundwater during rainfall was represented by pore water pressure. However, in relatively large rocks, hydrostatic water pressure and uplift pressure were still jointly applied. The resultant process of a laminated rockslide would be an accumulation slide.

Analysis of rapid and long run-out slide process

In Southern China, it is a very typical disaster mode that a rockslide triggered by a heavy rainfall is transformed into a rapid and long run-out debris flow (Yin 2011). Xu et al. (2012) reported a catastrophic avalanche–debris flow that was triggered by the heavy rainfall on July 27, 2010 in Sichuan. A mass of strongly weathered basalts with a volume of 480,000 m³ was initiated from a valley side slope and then moved downstream along the valley, entraining a large amount of unconsolidated substrate and

bilateral materials and colluviums. The entrainment increased the volume of slide to 1.0 million m³ and may also enhance the mobility of the rockslide. Zhang et al. (2011) conducted a study on the transform mechanism from rockslide to debris flow with ring shear test that indicated the so-called "soft base" effect. Because of shearing shrinkage, grain crushing, and layering, the sliding body volume of soil reduces in the course of shearing, which makes excess pore water pressure increase, and thus its shear strength decreases. Simultaneously, a thick liquefied layer is formed at the bottom of sliding body, of which thickness increases with shearing displacement increasing. The liquefied layer carries the sliding body moving fast and reduces its stability greatly. There is a different slide-flow transferring process between the Sanxicun rockslide and above cases. The Sanxicun rockslide had no obvious liquefied layer. After sliding, the rockslide at front edge was subject to shear failure, impacted, and then shoveled the surface rock, soil, and vegetation. With the increase in sliding volume, the rockslide flooded into the valley and merged into a mountain flood to form a debris flow. Hungr (2010) proposed a variety of rheological relations and developed the DAN-W rockslide dynamic analysis software to simulate this process. DAN-W is an MS Windows-based program used to model the post-failure motion of rapid rockslides. The basic premise of the analysis is that, as a result of sliding or other failure, a predefined volume of soil or rock ("the source volume") changes into a fluid and runs downslope, following a path of a defined direction and width. The mass can entrain additional material from the path and eventually deposits, when it reaches slopes that are sufficiently flat

Table 1 Calculating results of factor of safety (FOS) with various depths of groundwater

	Groundwater		FOS	
	Depth h (m)	h/H[a]	State 1[b]	State2[c]
1	0.0	0.0	1.105	1.105
2	10.8	0.2	1.079	1.015
3	21.6	0.4	1.033	0.907
4	32.4	0.6	1.007	0.819

[a] Ratio of depth between ground (h) and crack (H)

[b] Hydrostatic pressure in rear crack

[c] hydrostatic pressure in rear crack+bottom uplift pressure along sliding plane

Fig. 18 Seepage analysis with hydrostatic and uplift pressure (creeping stage)
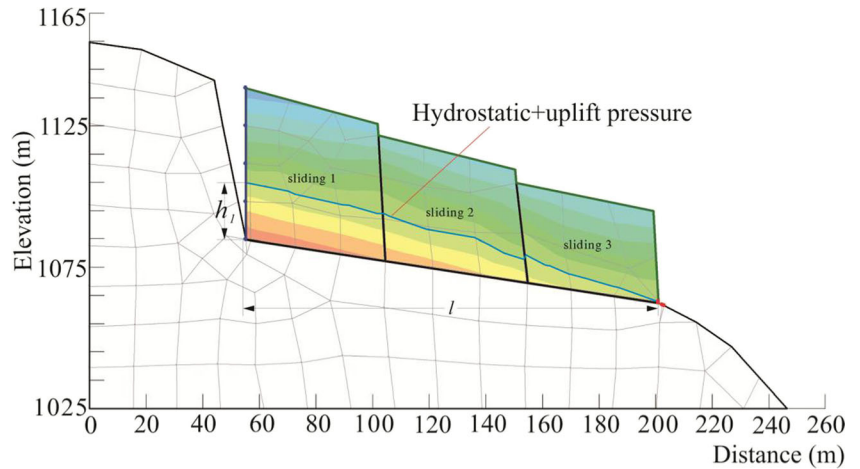
("the deposition area"). The model implements a one-dimensional Lagrangian solution of the equations of motion and is capable of using several alternative rheological relationships. Hungr's method simplifies the complicated sliding structure into a kind of equivalent fluid. The method assumes that the movement of rockslides are a shallow flow approximately similar to a parallel sliding bed with smaller sliding thickness. The sliding mass is divided into a certain number of mutually contacted blocks under curvilinear coordinates. These blocks can freely transform but have constant volume during movement. Through the Lagrange method, continuous equations and momentum equations are resolved on the basis of curvilinear coordinates and moving meshes. In the DAN method, Hungr (1995) took into

a No pressure head within fractures

b Pressure head within fractures(h1=h2)

Fig. 19 Seepage analysis with hydrostatic and uplift pressure (separating stage)

account factors such as terrain limits on both sides of the sliding approach and the internal strength of the sliding mass.

Establishment of model

The Double rheology model (F-V model for short) is based on a friction criterion and Voellmy criterion. It is established per the difference in ground rocks and divisions of sliding approach. In the F-V model, the rheological relation is based on the friction criterion for the impact-shoveling area but on the Voellmy criterion for the debris flow section (Hungr 2008; Hungr and Evans 2004), of which:

a. The bottom rockmass from rockslide shear failure at a high-level position in an impact-shoveling area is simulated using the friction criterion. The friction criterion is a rheological criterion with a single variable and its shear-resistant stress can be determined through the equation:

$$\tau = \sigma(1-r_{\mathrm{u}})\tan\phi$$

where τ stands for shear stress at the bottom of the sliding mass, σ stands for the overall stress in the vertical direction of sliding approach, r_{u} stands for the ratio of pore water pressure to normal stress and is normally assumed to be constant, and ϕ stands for friction angle. While using the friction criterion and taking into account the fractured rockmass after earthquake, the value of ϕ must tend to be lower than the normal value.

b. After sliding into the valley, the rockslide is transformed into a debris flow. Therefore, the Voellmy criterion is used to simulate the corresponding process. The shear stress resistance of the Voellmy criterion can be determined by the equation:

$$\tau = \sigma f + \rho g \frac{\upsilon^2}{\xi}$$

where f stands for the friction coefficient, ρ stands for the density of the sliding mass, g stands for gravitational acceleration, υ stands for the mean velocity of the sliding mass, and ξ stands for turbulivity (its value is the square of the Chézy coefficient). The f
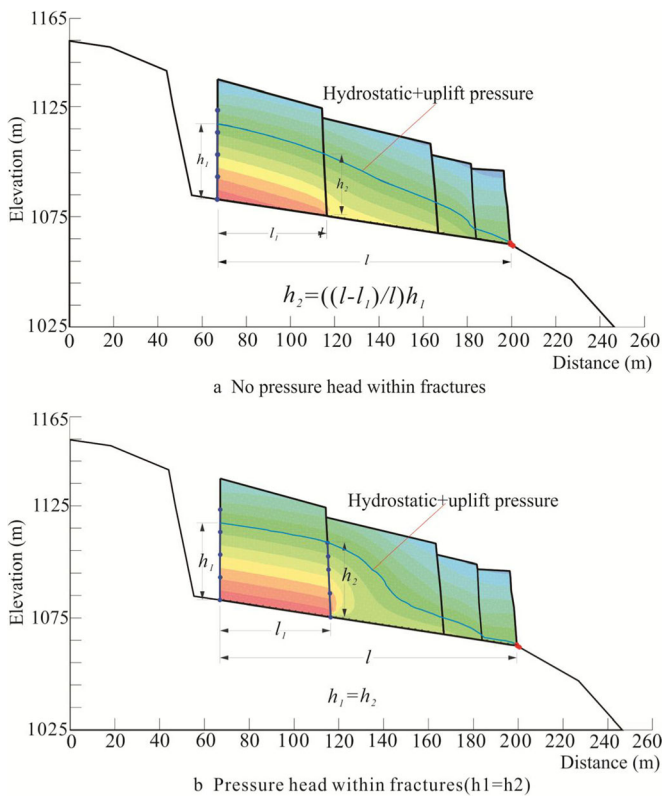
Table 2 Calculating results of sactor of safety (FOS) vs. different shapes of bottom uplift pressure with various depths of groundwater

| | Groundwater | Factor of Safety | |
	h/H^a (%)	$h_2=(l-l_1)h_1/l^b$	$h_2=h_1^c$
1	0.0	1.079	1.079
2	0.2	1.013	1.000
3	0.4	0.969	0.938
4	0.6	0.950	0.916

[a] Ratio of depth between ground (h) and crack (H)

[b] Triangle-shaped distribution of uplift pressure, h_2=water pressure head at l_1

[c] Rectangular-shaped distribution of uplift pressure, h_2 at $l_1=h_1$ at rear crack

and the ξ, are the two parameters to be determined when using this criterion.

The research and analysis on the dynamic and movement processes of rockslides are still in the early exploration stage. Hungr and Evans (2004) indicated that the results of the calculations were entirely dependent upon the data provided by the user. Therefore, persons using the program to make run-out estimates should be geoscience professionals thoroughly familiar with rockslides, soil and rock material behavior, and rheology, who have studied recent research publications on rockslide dynamics, including the relevant references listed at the end of this manual. The properties entered into the program should always be checked by back-analysis of real rockslide case histories, similar to the existing or potential rockslide being studied. The results of the analysis should never be relied on exclusively, but should be interpreted carefully by a qualified person in the light of field observations, empirical estimates, other analyses, and appropriate judgment and experience. Hungr and Evans (2004) held that its analysis via computation results was completely dependent on the data provided. Therefore, this paper adopts a trial-and-error method and references the research outcomes from Hungr and McDougall (2009) and Qi et al. (2012) to comprehensively investigate the movement process of the Sanxicun rockslide. Based on this and compared with the analysis results from paragraphs of "Basic characteristics of rockslide," we propose the rheology parameters of the F-V model as follows:

Internal friction angle of single variable for the friction criterion: $\phi=20°$

Friction coefficient: $f=0.21$ and turbulivity: $\xi=200$ m/s^2 in the Voellmy criterion

It is noteworthy that the friction criterion is applied, and the internal friction angle $\phi=25°$ at the area where houses were destroyed by the debris flow.

Analysis of simulation results

Run-out distance and accumulation

Figure 20 shows the movement status of the sliding mass under different simulations by the F-V model. After a shear failure 300 m away from original location (also see Fig. 7), the front edge of the sliding mass took 47 s to arrive at a location 1100 m away from original location. Due to the application of water flow in the valley,

it continued to move forward for 40 s and stopped 1250 m away from the original location.

The rockslide with a volume of 276,000 m^3 was subject to shear failure in a high-level position, moved forward 400 m, and then shoveled down the slope surface to a depth of 2 m with a total
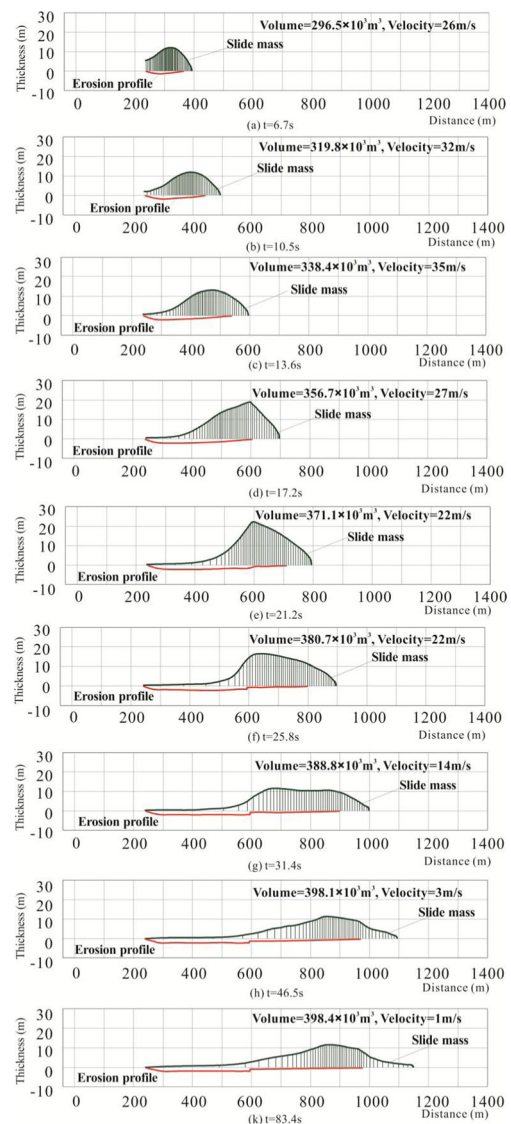

Fig. 20 Scenario of 2D depth profile of rockslide-debris run-out at Sanxicun

volume of 296,500 m³ (Fig. 20a). When moving forward 500 m, the rockslide continued to shovel down the slope surface to a depth of 2–3 m with a resultant volume of 319,800 m³ (Fig. 20b). When moving forward 600 m, a shoveling zone with a length of 250 m and depth of 1–3 m was formed, and the resultant volume of the rockslide increased to 338,400 m³ (Fig. 20c).

The rockslide converged with the flood in the valley at 600 m to form a debris flow and continued to move forward. When moving forward 700 m, the mud level in the confluence was as high as 18 m with a volume of 356,700 m³ (Fig. 20d). When it arrived at 800 m, the mud level in confluence was as high as 22 m with a volume of 371,100 m³ (Fig. 20e). When it arrived at 800–1000 m, houses were destroyed, and the volume increased to 388,800 m³ (Fig. 20f, g). Subsequently, the debris flow continued to move downward and the mud height in the confluence decreased from 17 to 12 m with a resultant volume of 398,400 m³ (Fig. 20h, k). The difference of the debris flow between the estimated volume of 360,000 m³ from the field observation and the calculated volume of 398,400 m³ based on the computer simulation is 38,400 m³. It should be noted that, when the water in debris flow was exhausted, the thickness of the solid accumulation was generally <8 m (Fig. 21, also see Figs. 10 and 11).

In general, after shear failure in a high-level position, the rockslide moved downward about 950 m in 47 s. When the rockslide moved forward 600 m, a shovel zone with a length of 250 m and depth of 1–3 m was created. Its volume increased to 338,400 m³, a debris flow was formed by its confluence with the flood of the valley, and the maximum height of the debris flow reached 22 m. When the rockslide arrived 800–1000 m away,
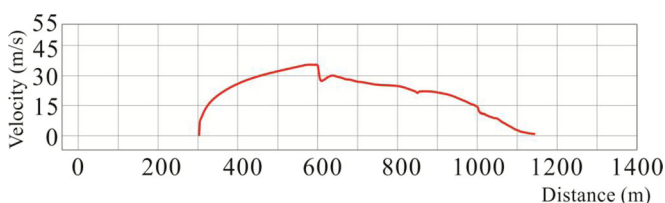

Fig. 22 Velocity of slide mass vs. distance of run-out of rockslide debris at Sanxicun

houses were destroyed with a resultant volume of up to 398,400 m³.

Movement velocity

If the initial velocity at the shear failure of the rockslide is set to zero, the sliding velocity kept increasing between 300 and 600 m (Fig. 22, also see Fig. 20). This sliding velocity reached a maximum value of 35 m/s at the location of 600 m with a movement time t=13.6 s. After entering the valley, the rockslide was transformed into a debris flow, and the corresponding velocity decreased to 28 m/s. At the distance of 800 m, the velocity before destroying houses was 22 m/s with a corresponding moving time of t=21.2 s and a time interval of Δt=21.2–13.6=7.6 s. Between the distances of 800 and 1000 m, 14 houses were destroyed, and the movement velocity decreased to 14.2 m/s with a corresponding moving time of t=31.3 s and a time interval of Δt=31.3–21.2=10.1 s. After that, the rockslide continued to move forward approximately 100 m with a corresponding moving time of t=46.7 s and a time interval of Δt=46.7–31.3=15.4 s. Finally, the rockslide tended to stabilize at 1250 m with a corresponding moving time of t=46.7 s and a time interval of Δt=83.4–46.7=36.7 s.

After shear failure occurred in a high-level position, the rockslide moved downward for approximately 950 m in 47 s with a maximum velocity of 35 m/s. This was a typical rapid and long run-out rockslide.

Discussions

Theoretically, the prediction and early warning on debris flows after earthquake is possible through the establishment on the critical precipitation to initiate debris flow after the earthquake. Quan et al. (2013) developed a model that could give a rough spatial and temporal prediction of expected change in landslide hazard in an area following an earthquake. The model is able to describe the reduced impact of earthquakes with distance from epicenter as well as how the soil gradually regains its strength with time. Yu et al. (2014) studied the ratio of rainfall thresholds after and before earthquakes in relation to the peak ground acceleration (PGA) of earthquakes and the number of rainy seasons after the

earthquake. The Wenchuan earthquake area is a mountainous area with height difference over several thousands of meters. The rainfall observation stations are very inadequate. Especially, there is almost no station in the initiation area to debris on the upper of the tributary. Existing researches on the initial threshold of rainfall is merely replaced by in the deposit area of debris at the month of the tributary. The "local effect on rainfall" is very obvious. The rainfall is much different in the various zones and the various elevations. That is why, so far, there is none of successful or reliable case of early warning to be reported on the above theory, ideal and method in the Wenchuan earthquake area. The method on critical precipitation to prediction/warning is not satisfied. A lot of fractured/cracked slopes that were resulted or intensified from the Wenchuan Ms 8.0 earthquake have similar geological conditions and structural characteristics as those associated with the Sanxicun rockslide. The early detection conditions of rockslide-debris flow disaster can be concluded as follows:

– Geology and geomorphology: The upper mountain is cracked by earthquake. A great deal of loose accumulation is in the middle valley. The lower valley contains villages in a relative flat terrain.
– Triggering factors: During a heavy rainfall, if the upper rockfall occurs, it would flood and erode the saturated accumulation in the valley and trigger the flow sliding to shovel loose accumulation. It can result in an increase in volume of sliding mass and creates a rapid and long run-out rockslide in a flow state.
– Hazard objects: The hazard objects include villages, roads, and bridges located in lower and relatively flat terrain.

The visible spectral remote sensing technique for early detection of landslides is difficult in this area due to the heavy vegetation coverage. The integration of field geological investigation with RS and InSAR is applied as an early detection tool (Zhao et al. 2013) to investigate the large-scale oblique dip apparent rockslide in the sliding source area. An outline of the detection method can be given as follows: (1) The tributary and cliff provide a free space for the apparent dip movement; (2) the block-fracture bedding structure is intercalated with weak layer as sliding plane; (3) the rockmass is split into obvious smaller, distinct blocks with several groups of large joints; (4) the sliding rockmass (i.e., the rockslide structure before movement) exists along a dip angle and is barricaded by an inclined stable bedrock area. The subsequent sliding direction is deflected from a true dip angle to an apparent dip angle. (5) The macrodeformation characteristics are obvious in and near the rockslide, such as small rockslide/fall and large crack/collapse, etc.

These indices can serve as a scientific consideration on which hazard regions can be classified and monitoring prevention can be established. Therefore, the early identification of adverse geological features in the potential landslide hazardous regions and hazard prevention (or mitigation) should be established on the basis of this disaster formulation as follows: (1) A high-resolution remote sensing and detail investigation must be applied to recognize the potential hazardous slope, (2) rainfall-based real-time monitoring stations are established on the source area of the rockslide-debris flow, (3) a safe siting work on the base of long run-out risk assessment is necessary to relocate and reconstruct, and (4) the

function for land-use should be changed. The strategic plan of the reconstruction of towns and villages in the Wenchuan Ms 8.0 earthquake area should address a limit on the scale of urban construction and plan appropriate areas, limited areas, and forbidden areas for construction. In the future, 5–10 years or even over a longer period, some ecological protection zones could be established to prevent damage to properties and reduce the number of casualties.

Conclusions

This paper uses the catastrophic rockslide at Sanxicun village, Dujianyan city as an example to investigate the characteristics of rapid and long run-out rockslide–debris flow from the cracked slopes intensified by the Wenchuan Ms 8.0 earthquake. This paper analyzes the stability of the cracked slopes after the Wenchuan Ms 8.0 earthquake, especially the instability mode under the condition of heavy rainfall. Four sliding stages of tension crack, creep sliding, separation, and residual accumulation under the application of hydrostatic water pressure and uplift pressure are discussed. Kinetic and dynamic processes of impact-shoveling area and debris flow are simulated. This paper summarizes the early detection signs of hazard objects and the geologic/geomorphic disaster characteristics, based on the rockslide-debris flow formation mechanisms at the Wenchuan Ms 8.0 earthquake area and heavy rainfall. These indices can serve as a scientific consideration for classifying hazard areas and monitoring for prevention of heavy rainfall type rockslides in earthquake areas.

Acknowledgments

References

Fan XM, Xu Q, Zhang ZY (2009) The genetic mechanism of a translational rockslide. Bull Eng Geol Environ 68:231–244
Feng Z, Yin YP, Li B (2012) Centrifuge modeling of apparent dip slide from oblique thick bedding rockslide. Chin J Rock Mech Eng 31(5):890–897 (in Chinese)
GEO-SLOPE International Ltd (2008) Stability modeling with SEEP/W 2007—an engineering methodology, 3rd edn. Calgary, Alberta
Hungr O (1995) A model for the run out analysis of rapid flow slides, debris flows, and avalanches. Can Geotech J 32:610–623
Hungr O (2008) Simplified models of spreading flow of dry granular material. Can Geotech J 45(8):1156–1168
Hungr O (2010) User's manual for DAN-W Dynamic analysis of landslides. 4195 Almondel Rd., West Vancouver, B.C., Canada, V7V 3L6
Hungr O, Evans SG (2004) Entrainment of debris in rock avalanches: an analysis of a long-runout mechanism. Geol Soc Am Bull 116:1240–1252
Hungr O, McDougall S (2009) Two numerical models for rockslide dynamic analysis. Comput Geosci 35:978–992
Ji SW, Zhang ZY, Liu HC (2000) The mechanism of deformation and failure for the slope composed of nearly horizontal competent and incompetent intercalated rock mass strata. Chin J Geol Hazard Control 11(9):49–53 (in Chinese)
Li YQ (1998) Master Zhang Daqian and Mt. Qiangcheng. Sichuan Today 11(4):32–34
Qi C, Xing AG, Yin YP (2012) Numerical simulation of Dynamic behavior of Donghekou rockslide–debris avalanche. J Eng Geol 20(3):334–339
Quan LB, Vangelsten BV, Liu ZQ, Eidsvig U and Nadim F (2013) Landslides induced by the interaction of an earthquake and subsequent rainfall. A spatial and temporal model. Proceedings of the 18th International Conference on Soil Mechanics and Geotechnical Engineering, Paris, pp 2237–2240
Tang C, Zhu J, Li WL, Liang JT (2009) Rainfall-triggered debris flows following the Wenchuan earthquake. Bull Eng Geol Environ 68:187–194

Tang C, Zhu J, Ding J (2011) Catastrophic debris flows triggered by a 14 August 2010 rainfall at the epicenter of the Wenchuan Ms8.0 earthquake. Landslides 8:485–497

Wang ZJ, Wang CG, Wang K (2012) Research on mechanism of rockslide of nearly horizontal soft rock slope caused by wedge-shape cracking expansionary force. J Railw Eng Soc No 12:36–41 (in Chinese)

Xu Q, Fan XM, Dong XJ (2012) Characteristics and formation mechanism of a catastrophic rainfall-induced rock avalanche–mud flow in Sichuan, China. Landslides 9:143–154

Yin YP (2011) Recent catastrophic landslides and mitigation in China. J Rock Mech Geotech Eng 3(1):10–18

Yin YP, Wang FW, Sun P (2009) Landslide hazards triggered by the 2008 Wenchuan Ms8.0 earthquake, Sichuan, China. Landslides 6(2):139–152

Yin YP, Sun P, Zhang M, Li B (2011) Mechanism on apparent dip sliding of oblique inclined bedding rockslide at Jiweishan, Chongqing, China. Landslides 8(1):49–65

Yu B, Wu YF, Chu SM (2014) Preliminary study on the effect of earthquake to the rainfall threshold of debris flows. Eng Geol. doi:10.1016/j.enggeo.2014.04.007

Zhang M, Yin Y, Hu R, Wu S, Zhang Y (2011) Ring shear test for transform mechanism of slide-debris flow. Eng Geol 118:56–62

Zhao X, Kang JW, Jiang J (2009) Strength index determine methods of the sliding zone soil in rockslide investigation. J Geol Hazards Environ Preserv 20(1):43–49 (in Chinese)

Zhao CY, Zhang Q, Yin YP, Zhong L (2013) Pre-, co-, and post-rockslide analysis with ALOS/PALSAR imagery data: a case study of Jiweishan rockslide, China. Nat Hazards Earth Syst Sci 13:2851–2861

Zhou W, Tang C (2013) Rainfall thresholds for debris flow initiation in the Wenchuan earthquake-stricken area, southwestern China. Landslides. doi:10.1007/s10346-013-0421-5

Y. Yin (✉) · **W. Wang**
China Institute of Geo-Environmental Monitoring,
Beijing, China
e-mail: yyueping@mail.cgs.gov.cn

Y. Cheng · **J. Liang**
Sichuan Geological Survey,
Chengdu, China